Electronic Supplementary Material (ESI) for Organic & Biomolecular Chemistry.

Supporting Information

Spiro-based Diamond-type nanogirds (DGs) via two ways of 'A_1B_1'/ 'A_2+B_2' type gridization of vertical spiro-based fluorenol synthons

Ying Wei,[†a] Yang Li,[†a] Dongqing Lin,[a] Dong Jin,[a] Xue Du,[a] Chunxiao Zhong,[a] Ping Zhou,[a] Yue Sun,[a] Linghai Xie,*[a] and Wei Huang[ab]

[a]Centre for Molecular Systems and Organic Devices (CMSOD), Key Laboratory for Organic Electronics and Information Displays & Jiangsu Key Laboratory for Biosensors, Institute of Advanced Materials (IAM), Jiangsu National Synergetic Innovation Center for Advanced Materials (SICAM), Nanjing University of Posts & Telecommunications, 9 Wenyuan Road, Nanjing 210023 (P.R. China).

[b]Shaanxi Institute of Flexible Electronics (SIFE), Northwestern Polytechnical University (NPU), 127 West Youyi Road, Xi'an 710072, Shaanxi, China

Table of contents

1. The structure of DGs-1, DGs-2, and their stereoisomers.

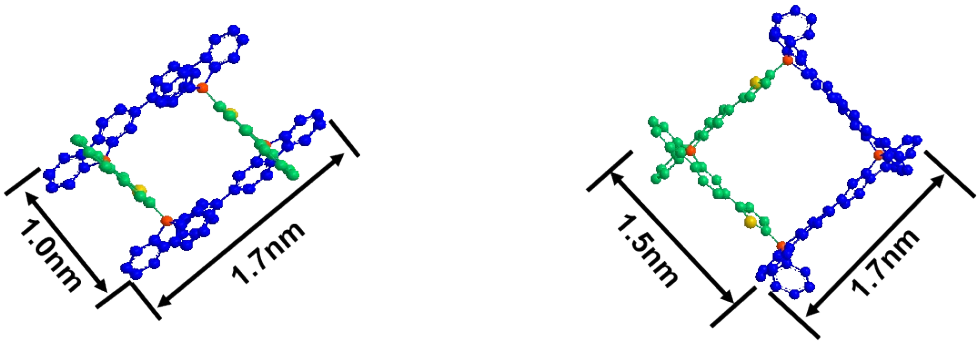

Diamond-type gridons-1 (DGs-1) **Diamond-type gridons-2 (DGs-2)**

Fig. S1 Two Diamond-type nanogirds' theoretical size, the substituents and hydrogen atoms are omitted.

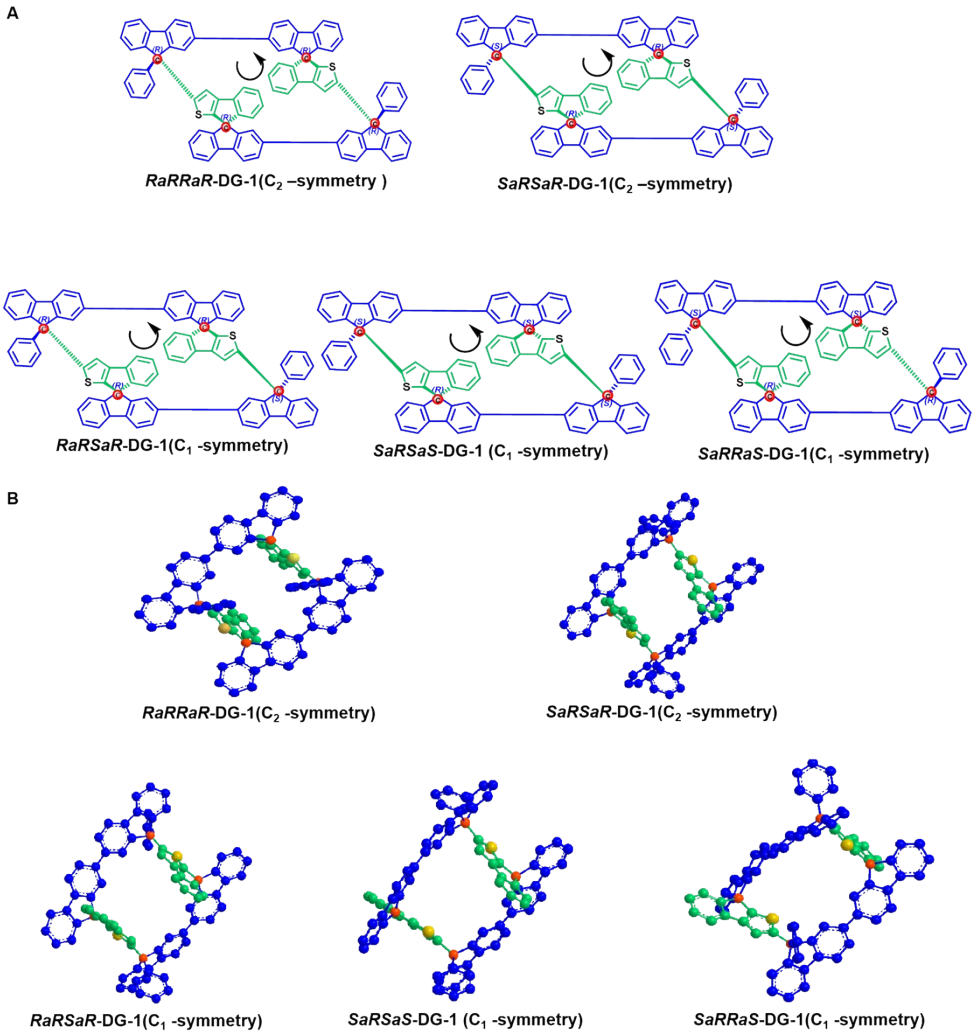

Fig. S2 The stereoisomers of DGs-1, the substituents and hydrogen atoms are

omitted. (A) displayed formula; (B) stereostructural formula.

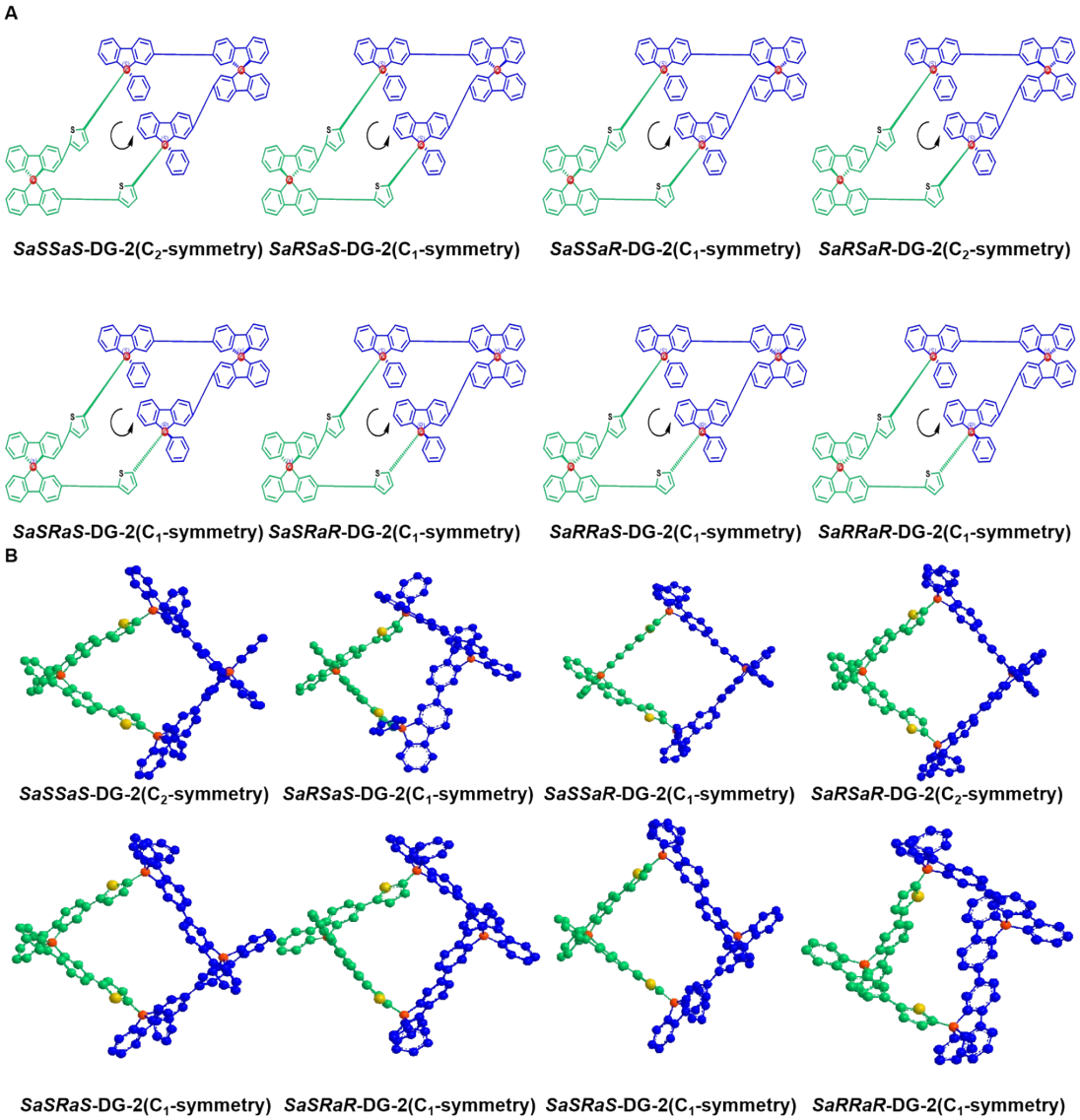

Fig. S3 The stereoisomers of DGs-2, the substituents and hydrogen atoms are omitted. (A) displayed formula; (B)stereostructural formula.

2. The theoretical calculation of DGs.

The strain energier of DGs-1 and DGs-2 were carried out by a homodesmotic reaction (Fig. S4) and the DFT calculation at the B3LYP/6-31G(d) level, and the results showing in Fig. S5, which indicate the easy synthesis of DGs-2.

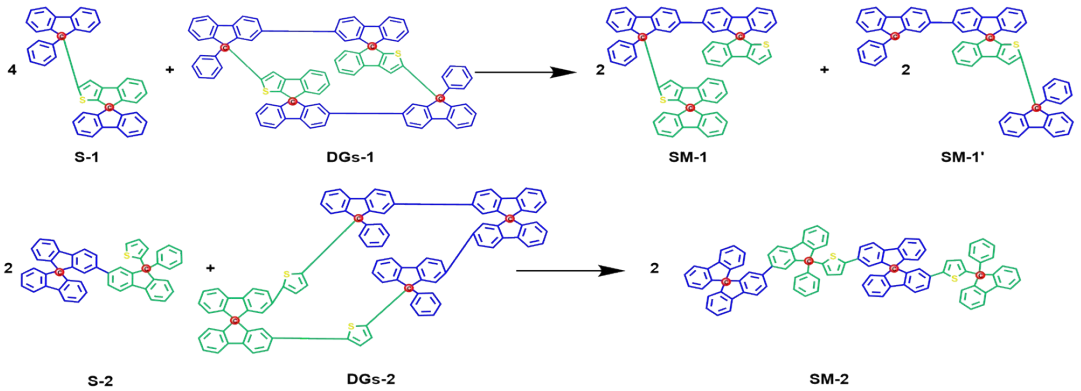

Fig. S4 The homodesmotic reactions of DGs-1 and DGs-2.

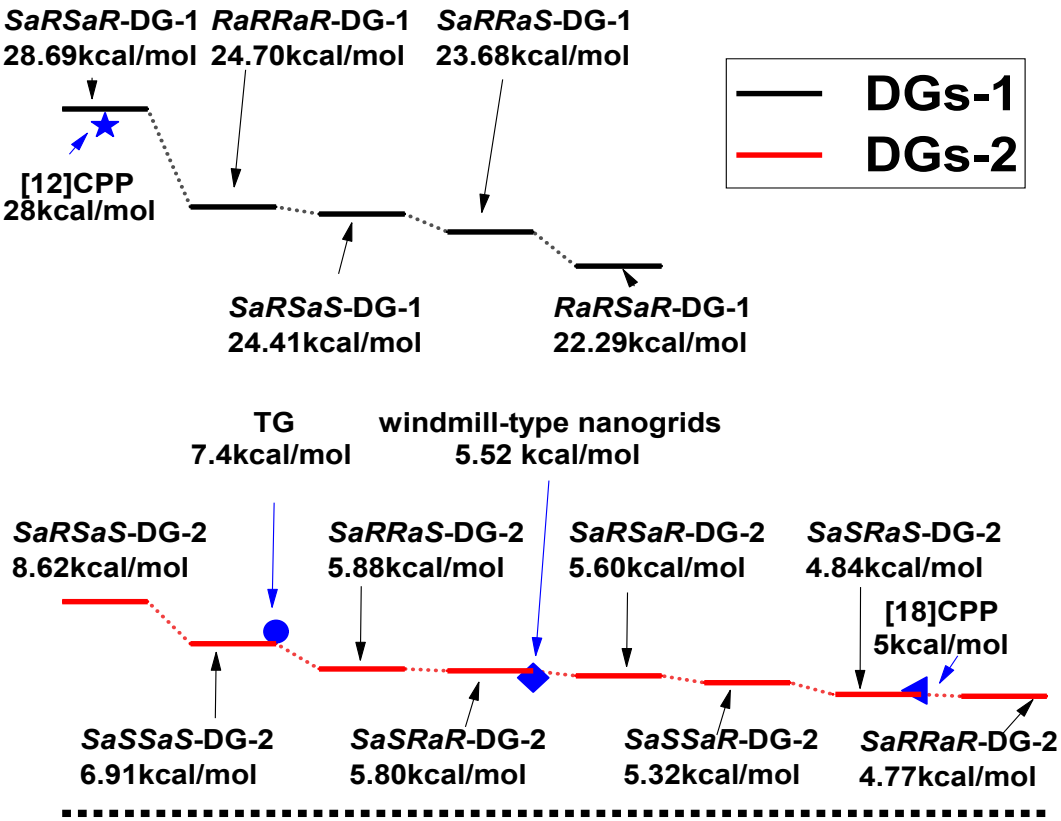

Fig. S5 The strain energies of DGs-1 and DGs-2.

3. The TLC, ^{1}H NMR and MALDI-TOF-MS spectrum of DGs' reaction mixtures.

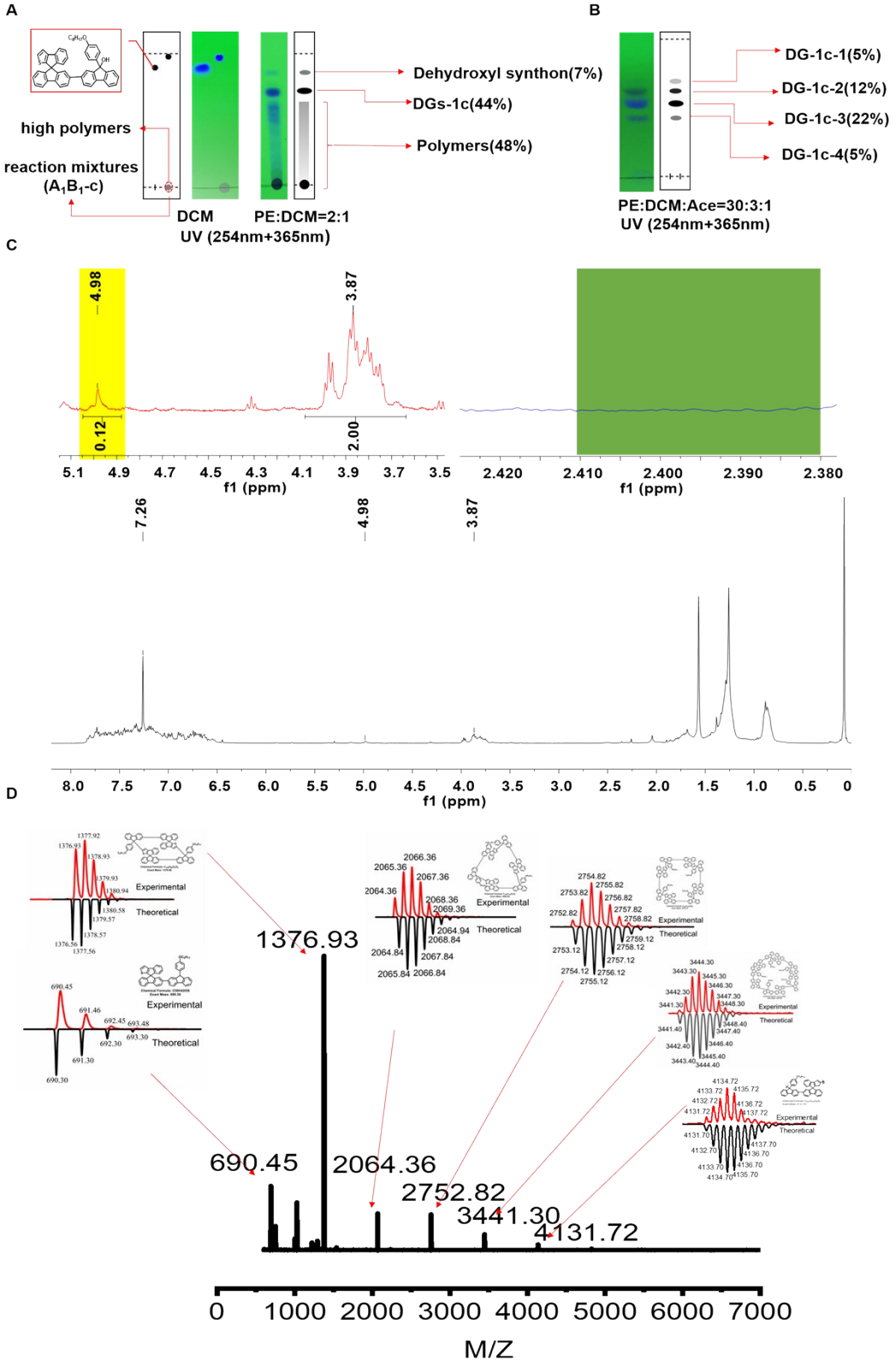

Fig. S6 (A) Photograph of the TLC chromatograms of the reaction mixtures of A_1B_1-c

under a UV lamp with irradiation wavelengths of 254 nm + 365 nm, the developing solvent is DCM (the A_1B_1 have completely reacted, consistent with a total yield of 98% and high polymers were found) or PE:DCM=3:1; (B) Photograph of the TLC chromatograms of the stereoisomers of DGs-1c; (C) The ^1H NMR (400MHz, $CDCl_3$) of reaction mixtures in A_1B_1-c, no significant OH absorption peak was observed during 2.38-2.41ppm (light green area) to indicate the A_1B_1-c has completely reacted, consistent with a total yield of 98%, the integral value is 0.12 (0.12>0.07) during 4.90-5.00ppm (yellow area) to indicate linear polymers; (D) The MALDI-TOF-MS spectrum of A_1B_1-c reaction mixtures, the byproducts, including dehydroxyl synthon and oligomers (the trimer grid, tetramer grid, pentamer grid and linear hexamer).

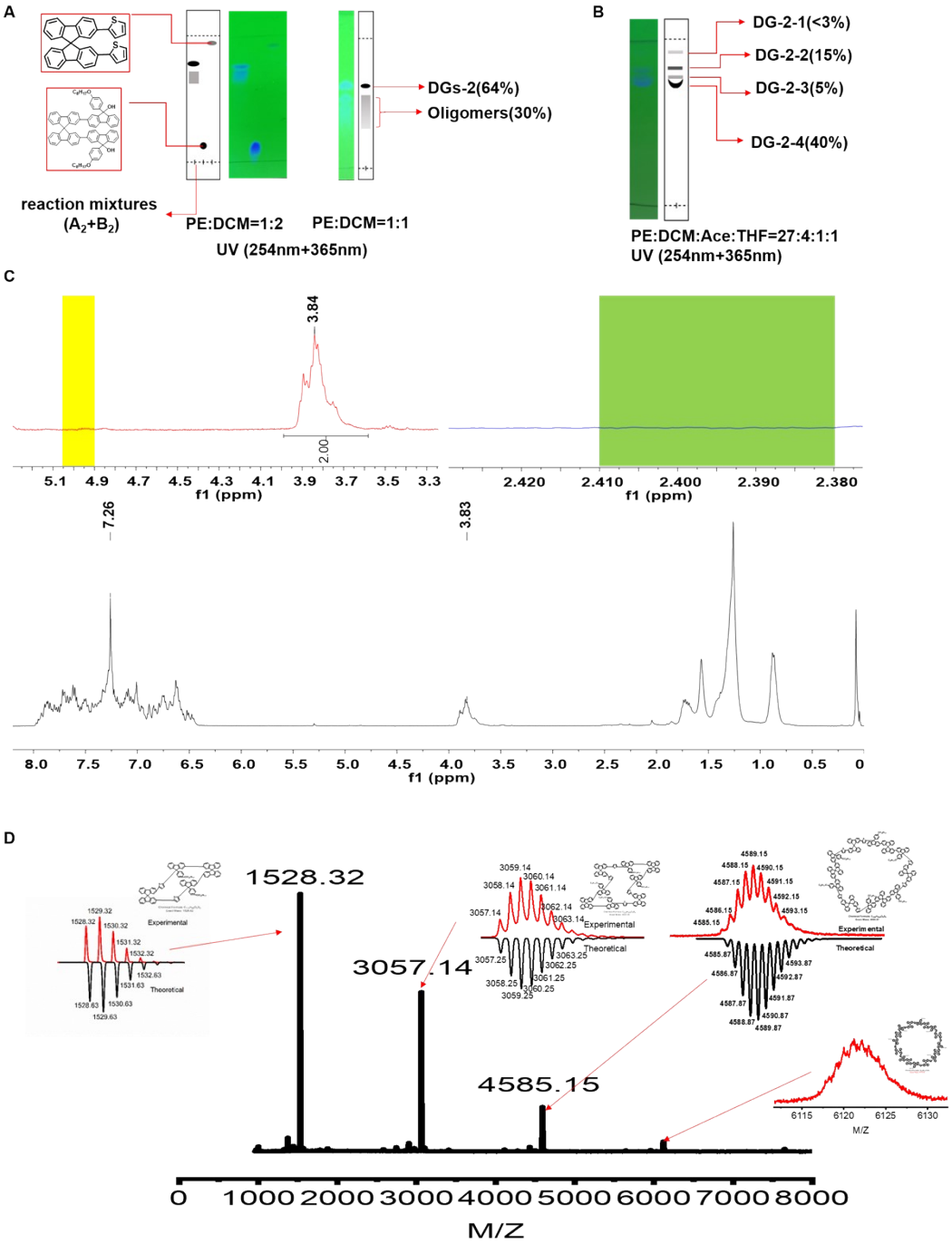

Fig. S7 (A) Photograph of the TLC chromatograms of the reaction mixtures of A_2+B_2 under a UV lamp with irradiation wavelengths of 254 nm + 365 nm, the developing solvent is PE:DCM=1:2 (the A_2+B_2 have completely reacted, consistent with a total yield of 94% and no high polymers were found) or 1:1; (B) Photograph of the TLC chromatograms of the stereoisomers of DGs-2; (C) The ^{1}H NMR (400MHz, $CDCl_3$) of reaction mixtures in A_2+B_2, no significant OH absorption peak was observed during 2.38-2.41ppm (light green area) to indicate the A_2 has completely reacted and no

significant absorption during 4.90-5.00ppm (yellow area) to indicate linear polymers without A_2 closure; (D) The MALDI-TOF-MS spectrum of A_2+B_2 reaction mixtures, the byproducts, oligomers (the dimeric grid, trimer grid, tetramer grid).

4. The GPC spectrum.

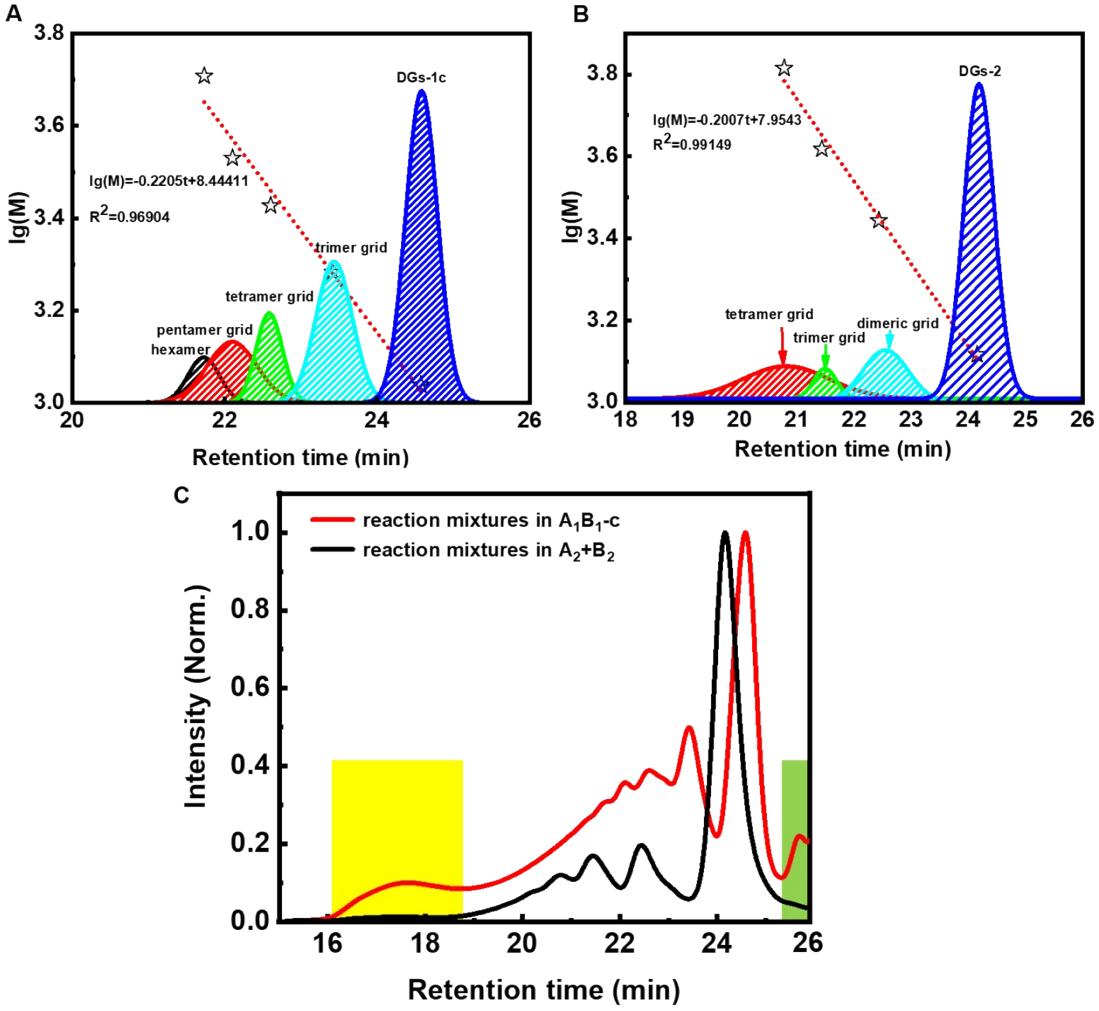

Fig. S8 (A) The calibration of DGs-1c and polymers (The blue, sky-blue, green, red, and black peaks correspond to DGs-1c, trimer, tetramer, pentamer, and hexamer, respectively, in which the star dots exhibit their individual logarithmic molecular mass lg M and retention time t), the coefficient of determination R^2 is 0.96904 (<0.99), indicates that the structure of all polymers is not consistent, hexamer is linear (Judge by the degree of deviation from the linear fitting function, consistented with Fig.S6D). (B)The calibration of reaction mixtures in A_2+B_2 (The blue, sky-blue, green, and red peaks correspond to DGs-2, dimer, trimer, tetramer, respectively, in

which the star dots exhibit their individual logarithmic molecular mass lg M and retention time t), the coefficient of determination R^2 is 0.99149 (>0.99), indicates that the structure of all products is consistent, that is, all are nonlinear. (C) The GPC spectrum of reaction mixtures in A_1B_1-c and A_2+B_2, high polymers (yellow area) and dehydroxyl synthon (green area) were found in A_1B_1-c (consistented with Fig.S6A and S7A).

5. The ^{1}H NMR spectra of the DGs and DGs' stereoisomers.

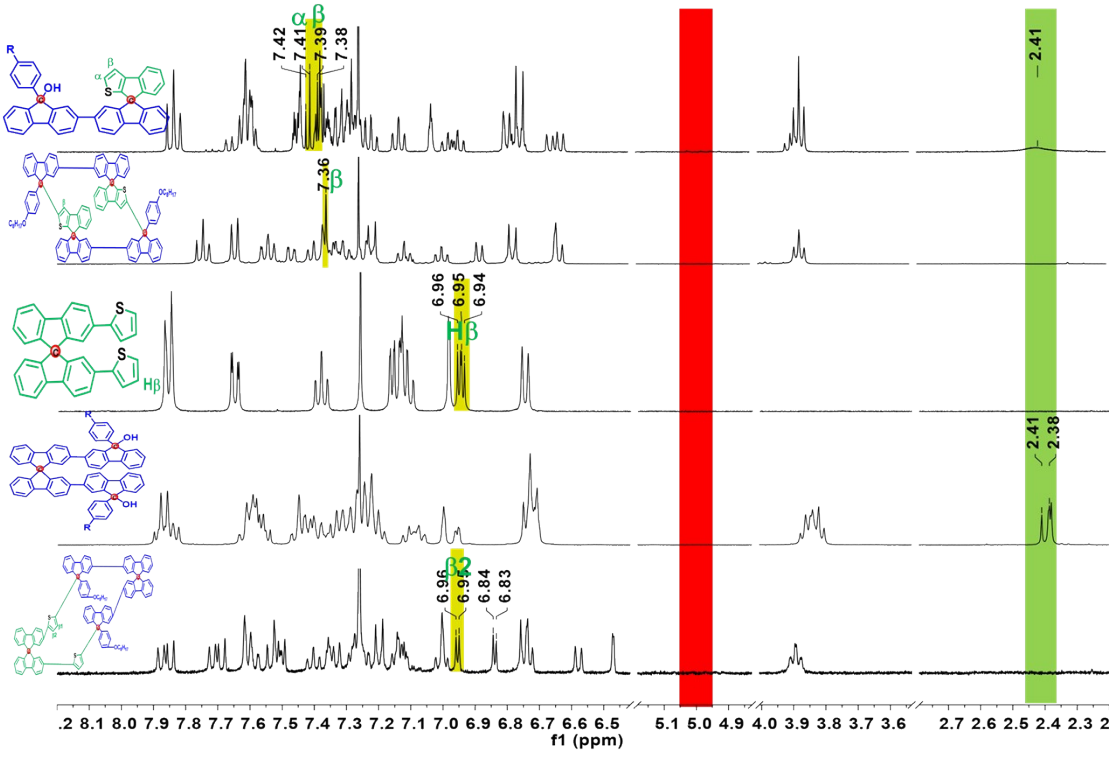

Fig. S9 The ^{1}H NMR spectrums (400MHz, $CDCl_3$) of A_1B_1 shaped synthon, DGs-1c, B_2 shaped synthon, A_2 shaped synthon, and DGs-2. The characteristic peaks of hydroxyl groups at 2.41-2.38 ppm disappear and the peak of hydrogen proton (4.90-5.00 ppm) at the 9 position of fluorene was not observed, and the changes protons on

thiophene, which clearly demonstrated the formation of grids.

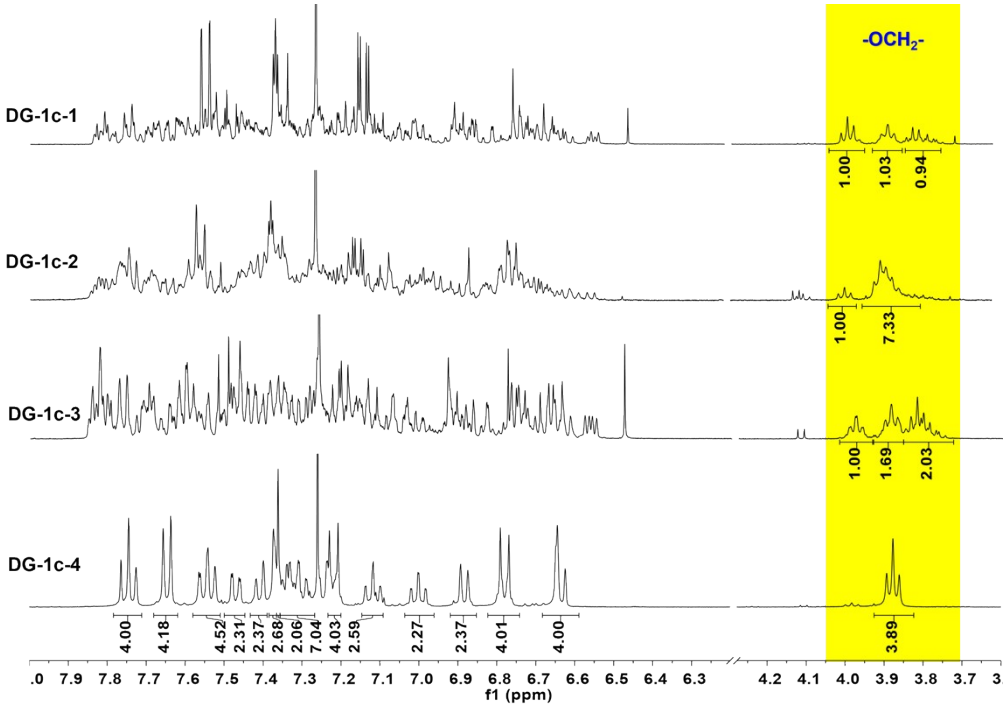

Fig. S10 The ^{1}H NMR spectrums (400MHz, $CDCl_3$) of DGs-1c, the sets of peaks or the ratio of hydrogens in 3.75-4.05 ppm (-OCH_2-, the yellow area) showed DG-1c-1, DG-1c-2 and DG-1c-3 were mixture.

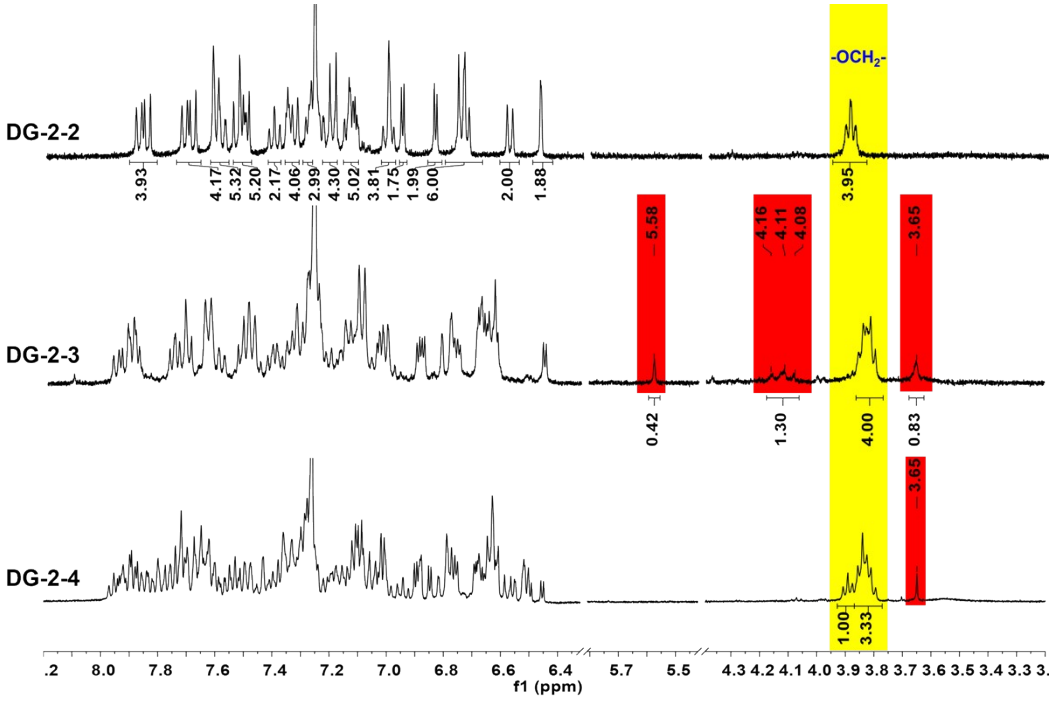

Fig. S11 The ^{1}H NMR spectrums (400MHz, $CDCl_3$) of **DG-2-2, DG-2-3 and DG-2-4.4.08**-4.16 ppm (1.3H, the red area), 3.65 ppm (0.8H, the red area) both proved that DG-2-

3 was a mixture. The ratio of hydrogens (1:3.33) in 3.75-3.95 ppm (OCH_2, the yellow area) revealed DG-2-4 was a mixture, too.

6. ^{1}H and ^{13}C NMR spectra of the compounds

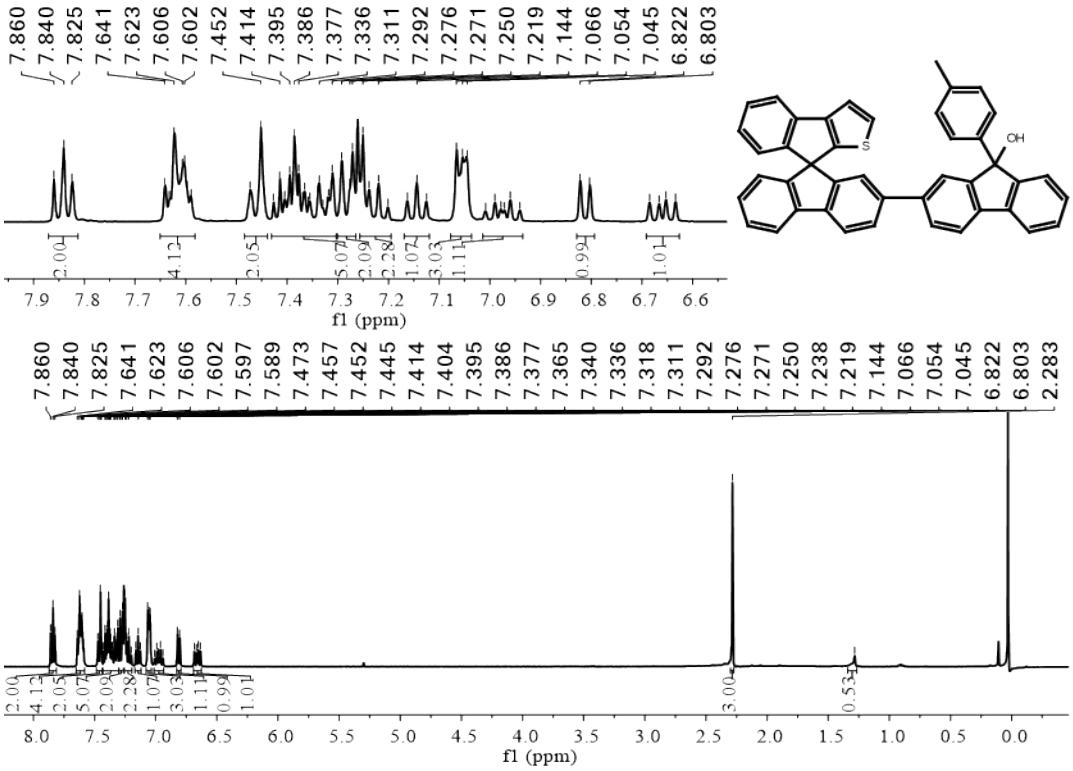

Fig. S12 ^{1}H NMR (400MHz, $CDCl_3$) spectrum of A_1B_1-a.

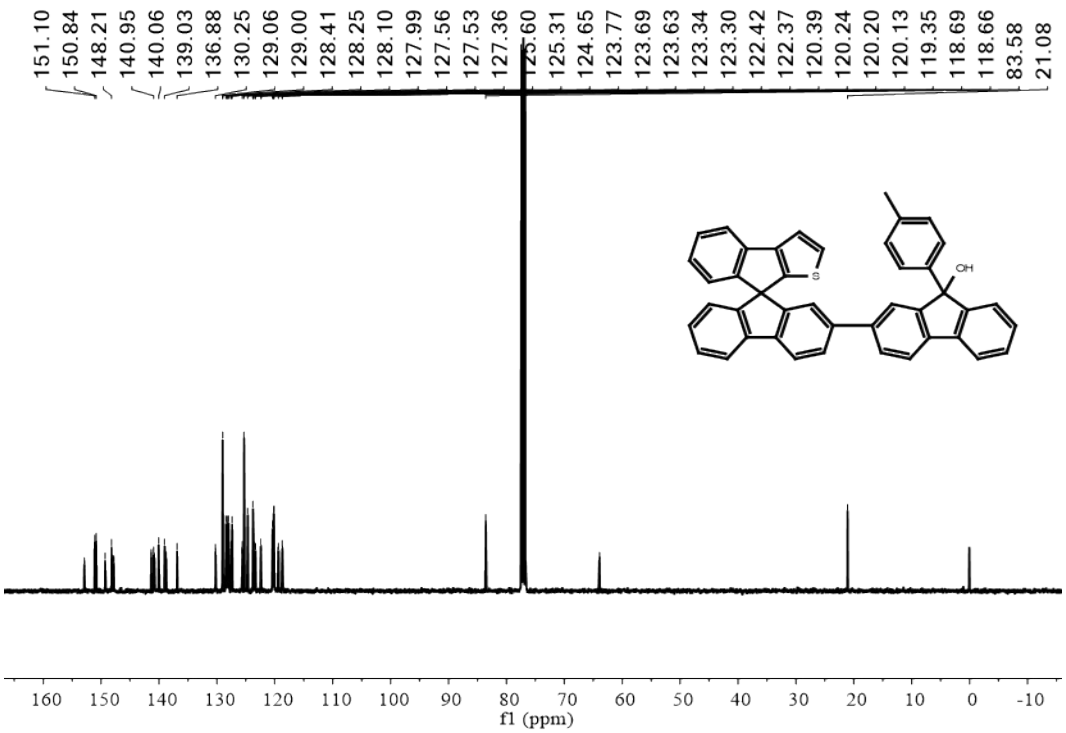

Fig. S13 ^{13}C NMR (100MHz, $CDCl_3$) spectrum of A_1B_1-a.

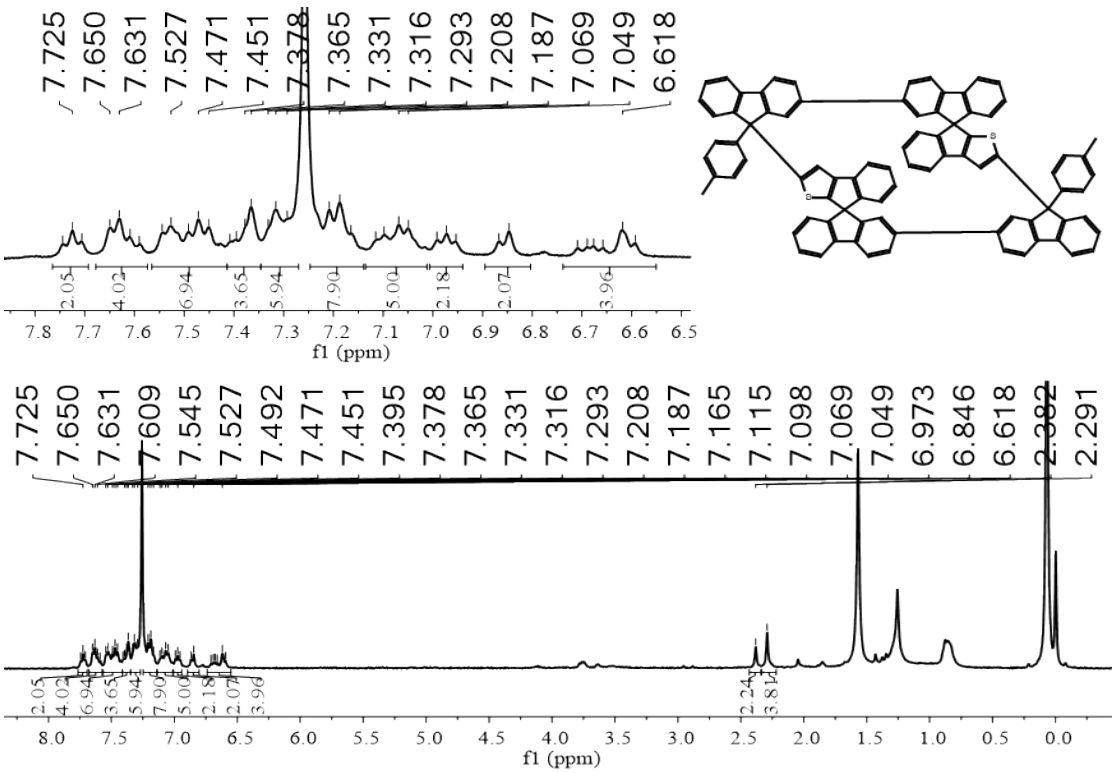

Fig. S14 ^{1}H NMR (400MHz, $CDCl_3$) spectrum of DGs-1a.

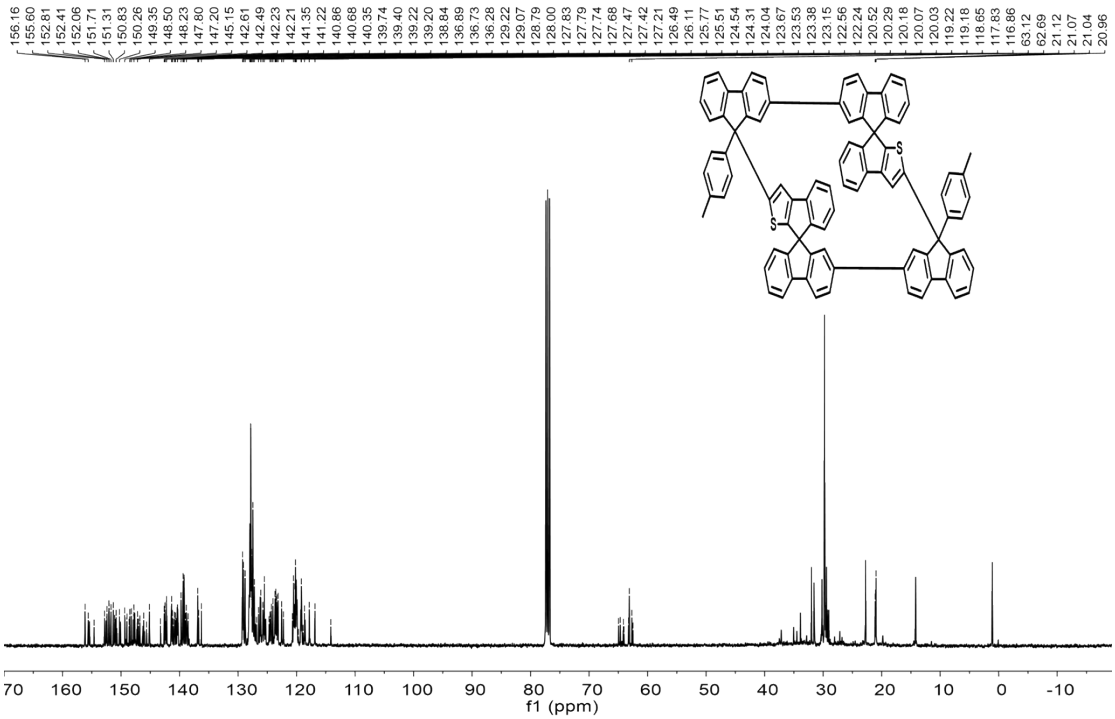

Fig.15 ^{13}C NMR (100MHz, $CDCl_3$) spectrum of DGs-1a.

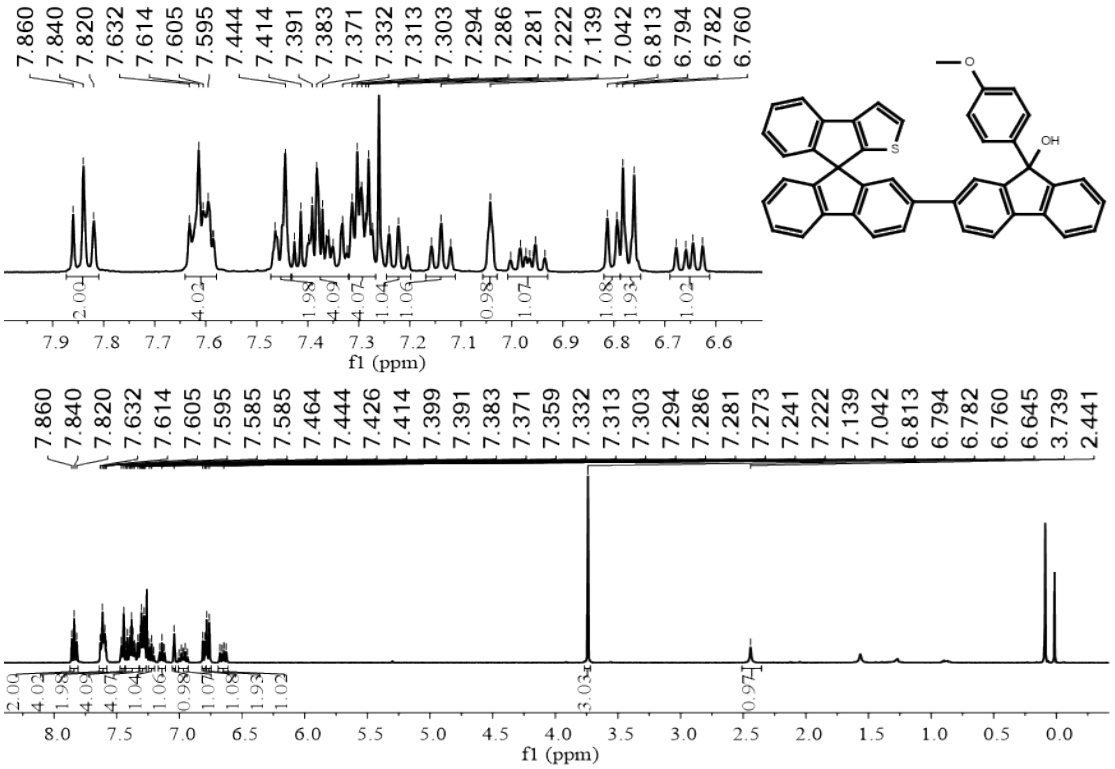

Fig. S16 ^{1}H NMR (400MHz, $CDCl_3$) spectrum of A_1B_1-b.

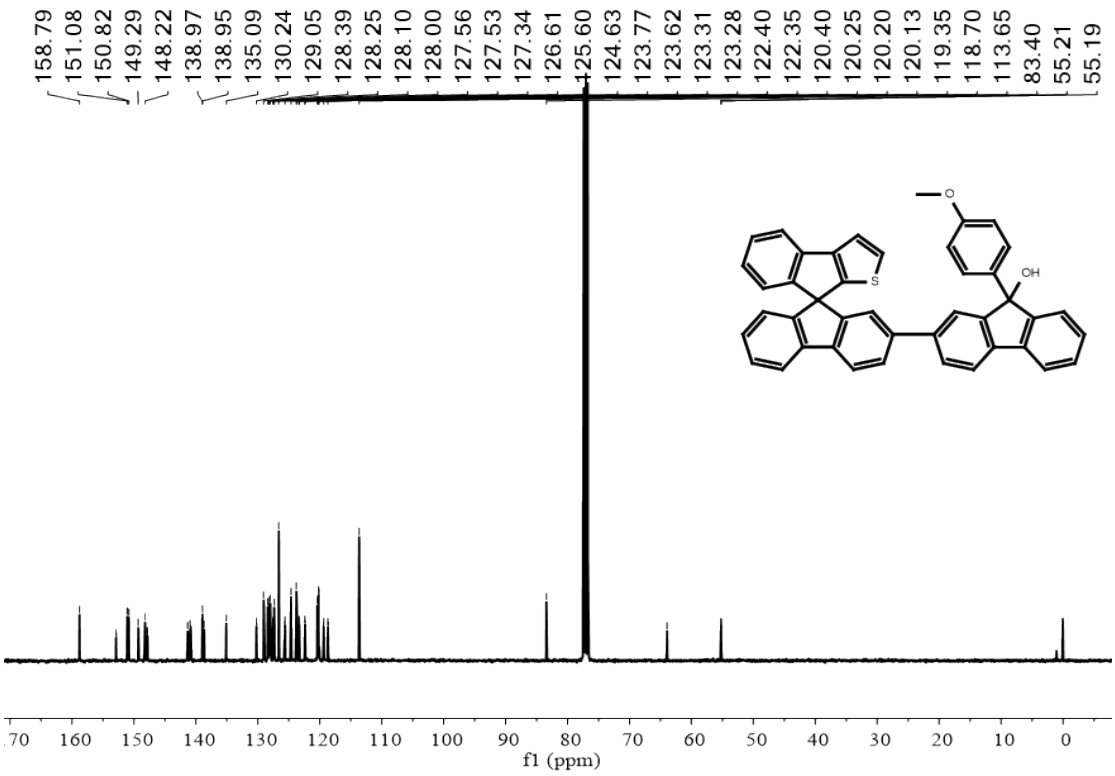

Fig. S17 ^{13}C NMR (100MHz, $CDCl_3$) spectrum of A_1B_1-b.

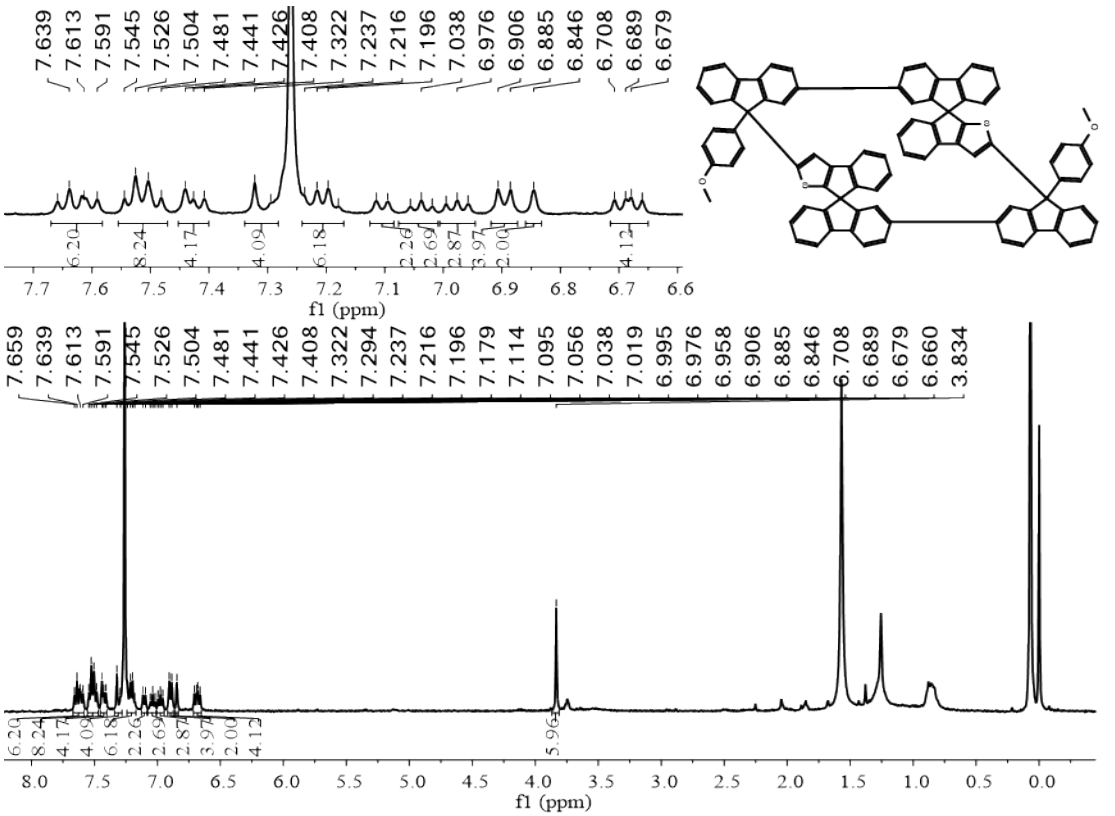

Fig. S18 ^{1}H NMR (400MHz, $CDCl_3$) spectrum of DGs-1b.

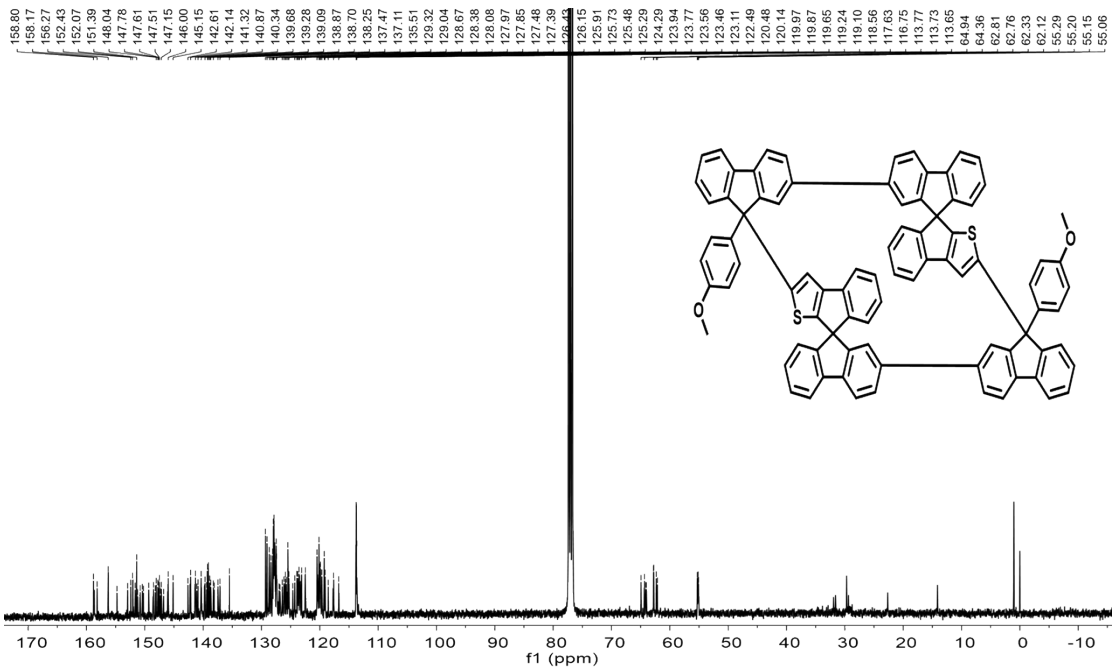

Fig. 19 ^{13}C NMR (100MHz, CDCl3) spectrum of DGs-1b.

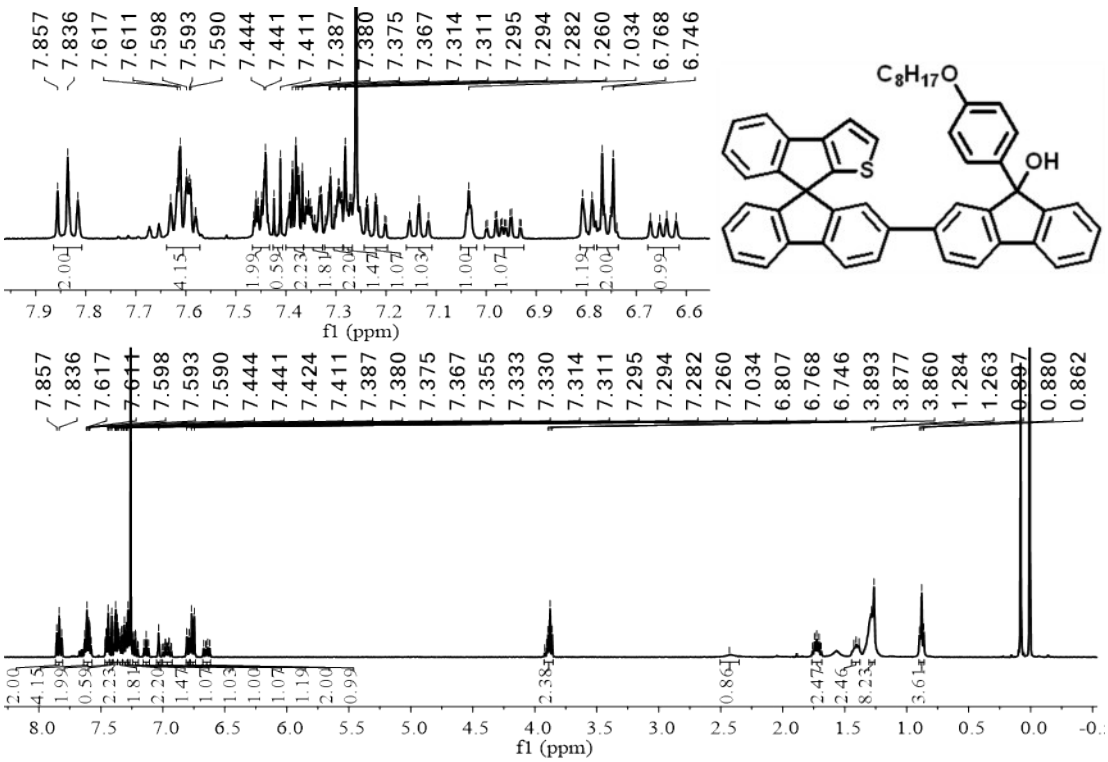

Fig. S20 ^{1}H NMR (400MHz, $CDCl_3$) spectrum of A_1B_1-c.

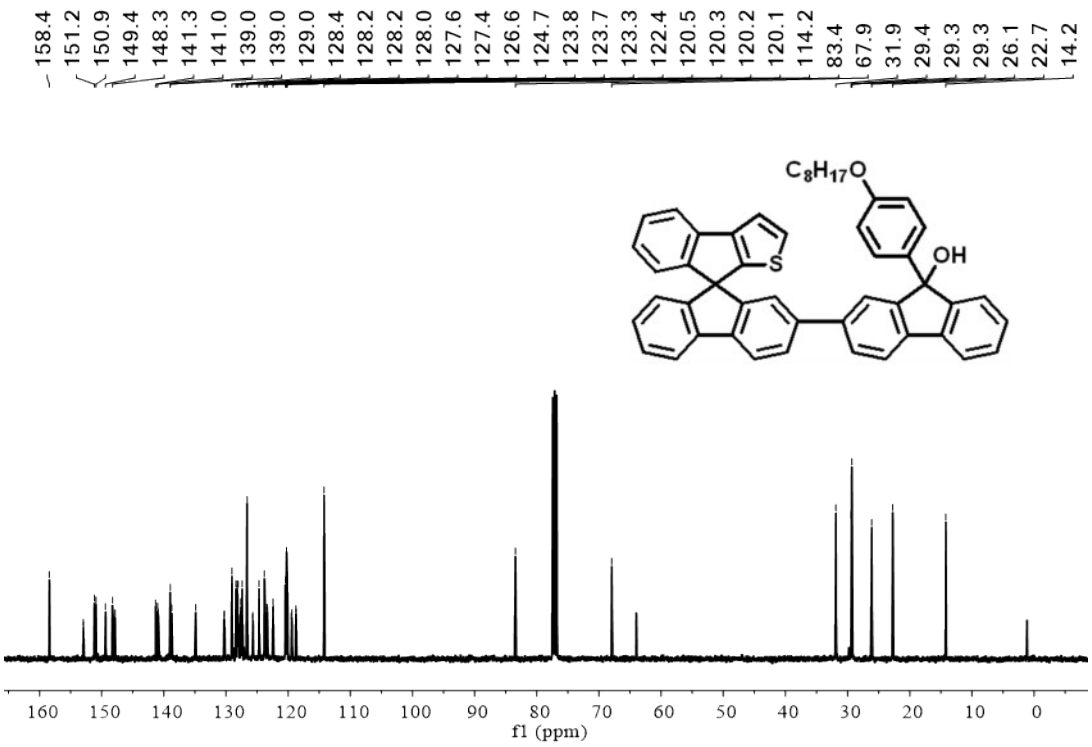

Fig. S21 ^{13}C NMR (100MHz, $CDCl_3$) spectrum of A_1B_1-c.

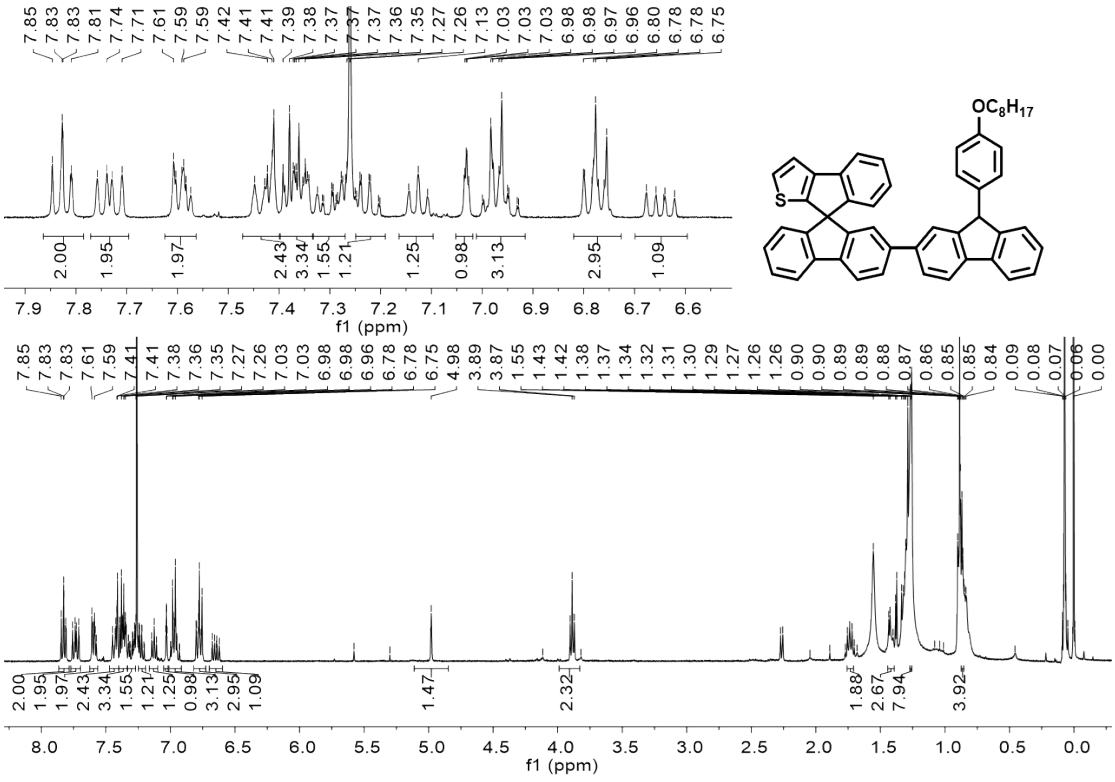

Fig. S22 ^{1}H NMR (400MHz, $CDCl_3$) spectrum of Ds-1c.

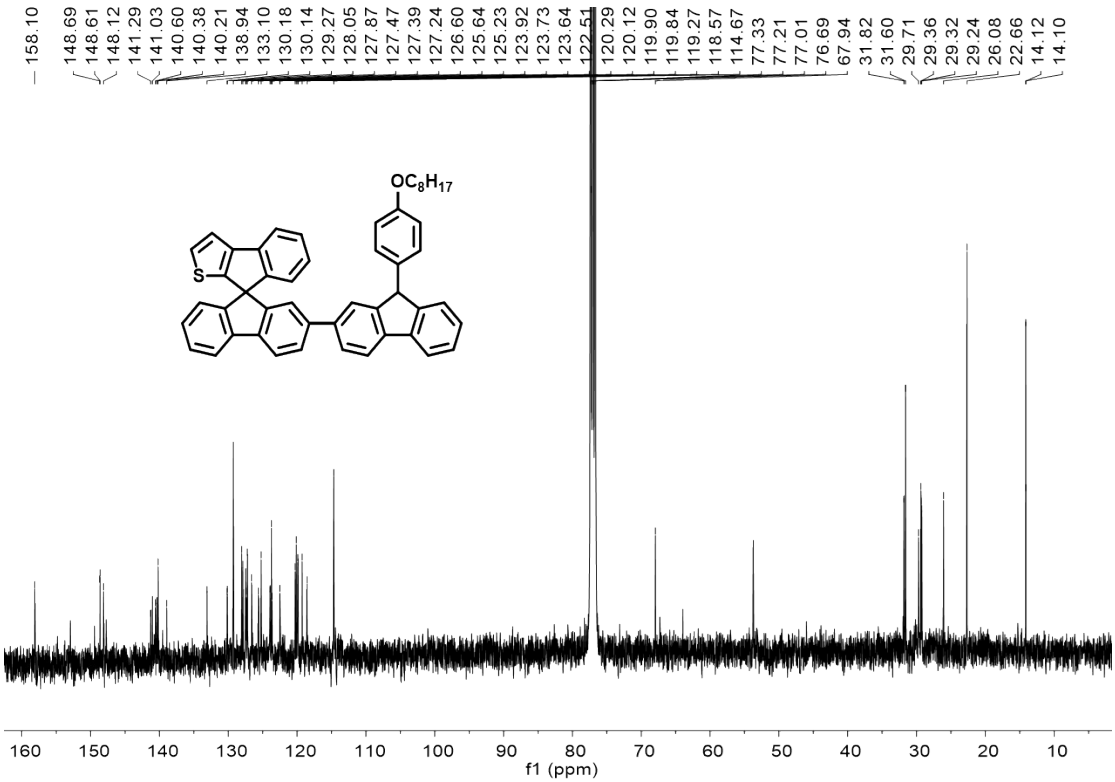

Fig. S23 ^{13}C NMR (100MHz, $CDCl_3$) spectrum of Ds-1c.

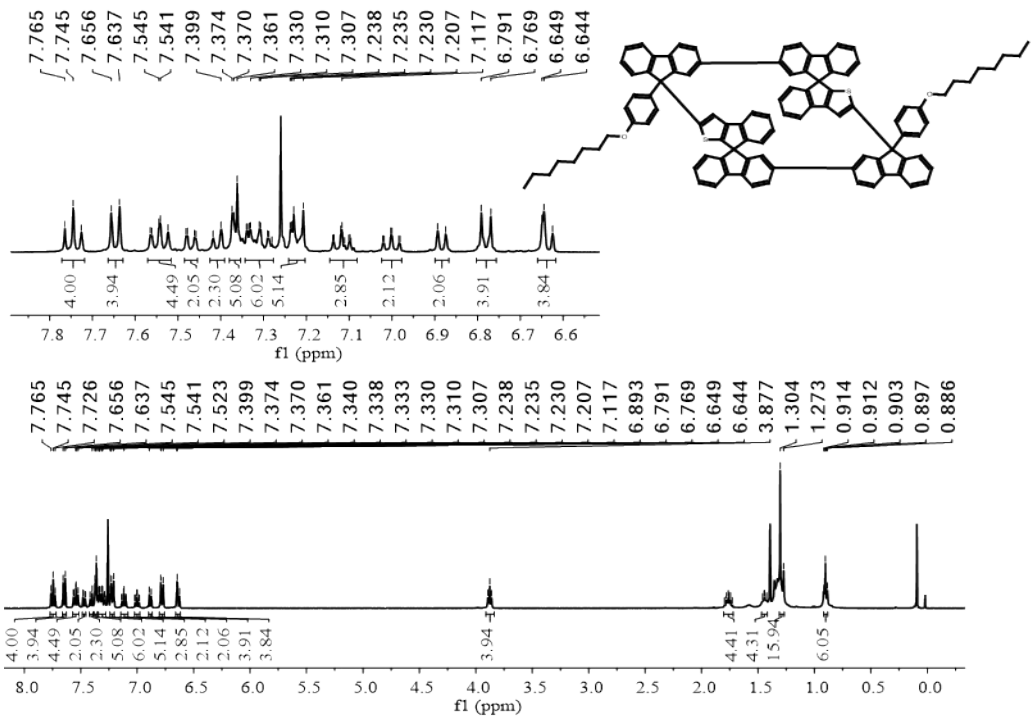

Fig. S24 ^{1}H NMR (400MHz, $CDCl_3$) spectrum of DGs-1c.

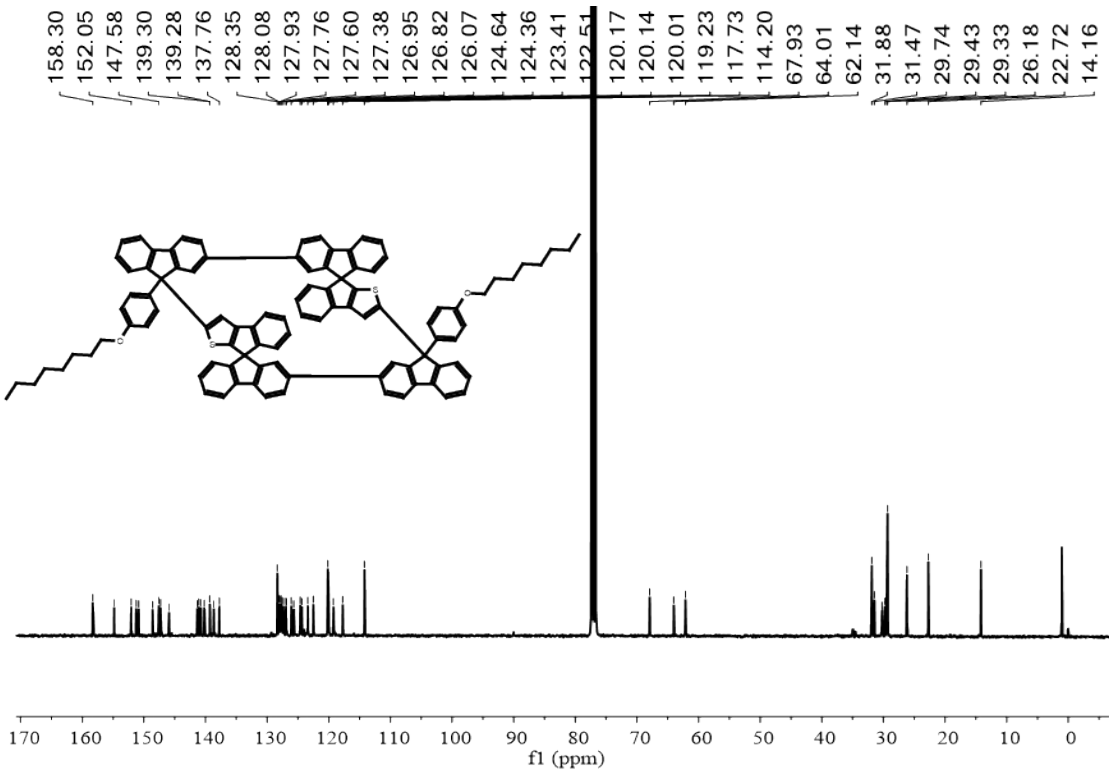

Fig. S25 ^{13}C NMR (100MHz, $CDCl_3$) spectrum of DGs-1c.

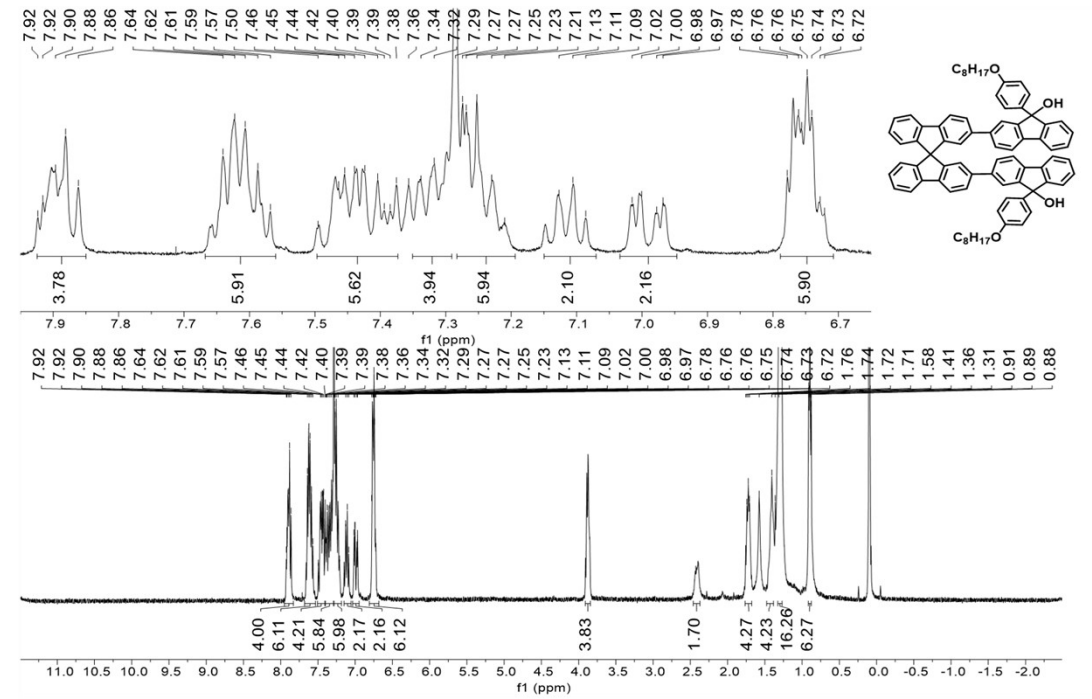

Fig. S26 ^{1}H NMR (400MHz, $CDCl_3$) spectrum of A_2.

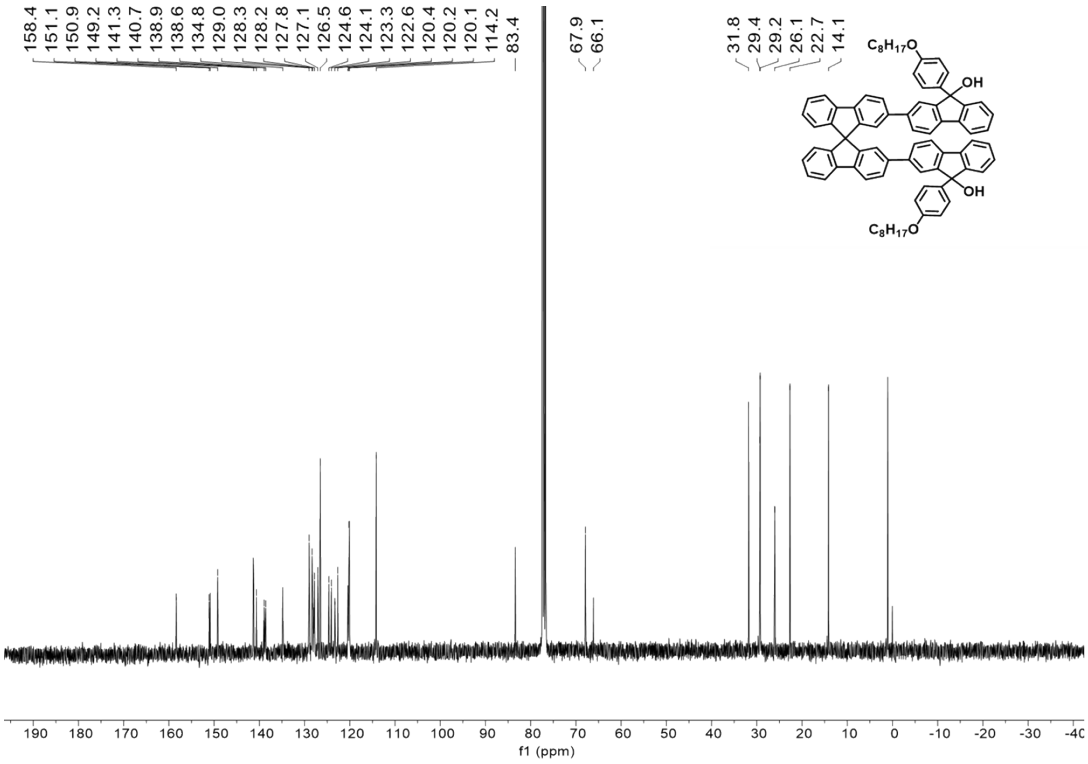

Fig. S27 ^{13}C NMR (100MHz, $CDCl_3$) spectrum of A_2.

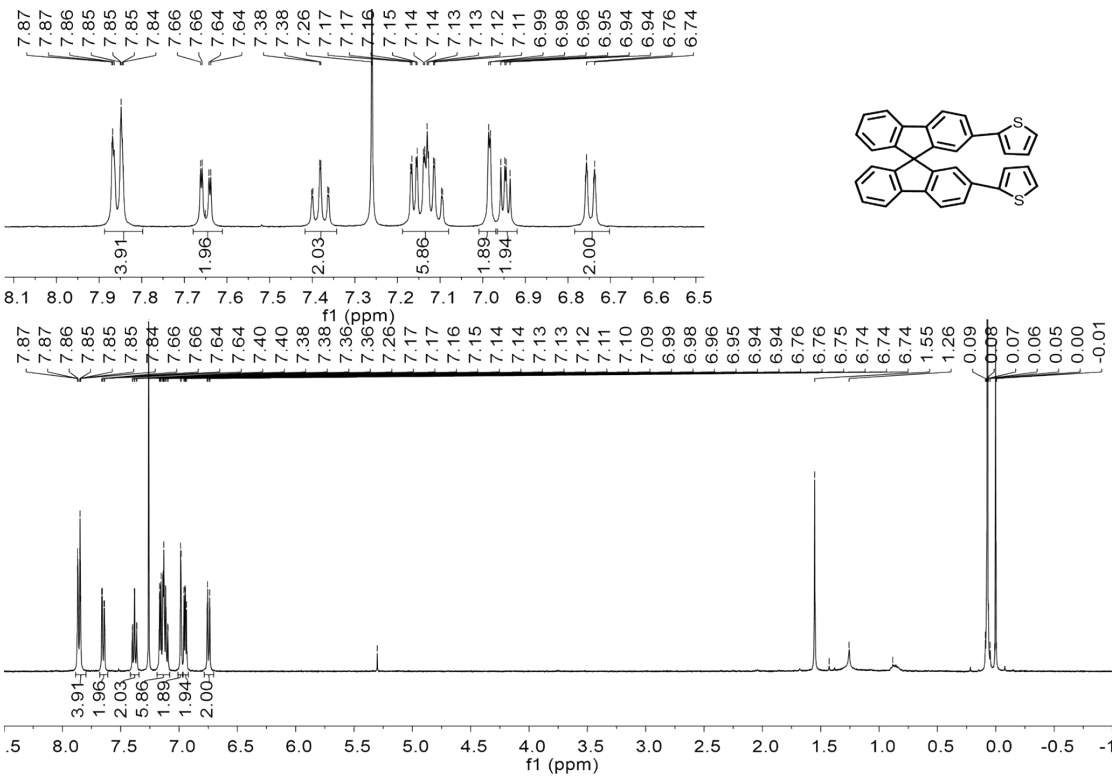

Fig. S28 ^{1}H NMR (400MHz, $CDCl_3$) spectrum of B_2.

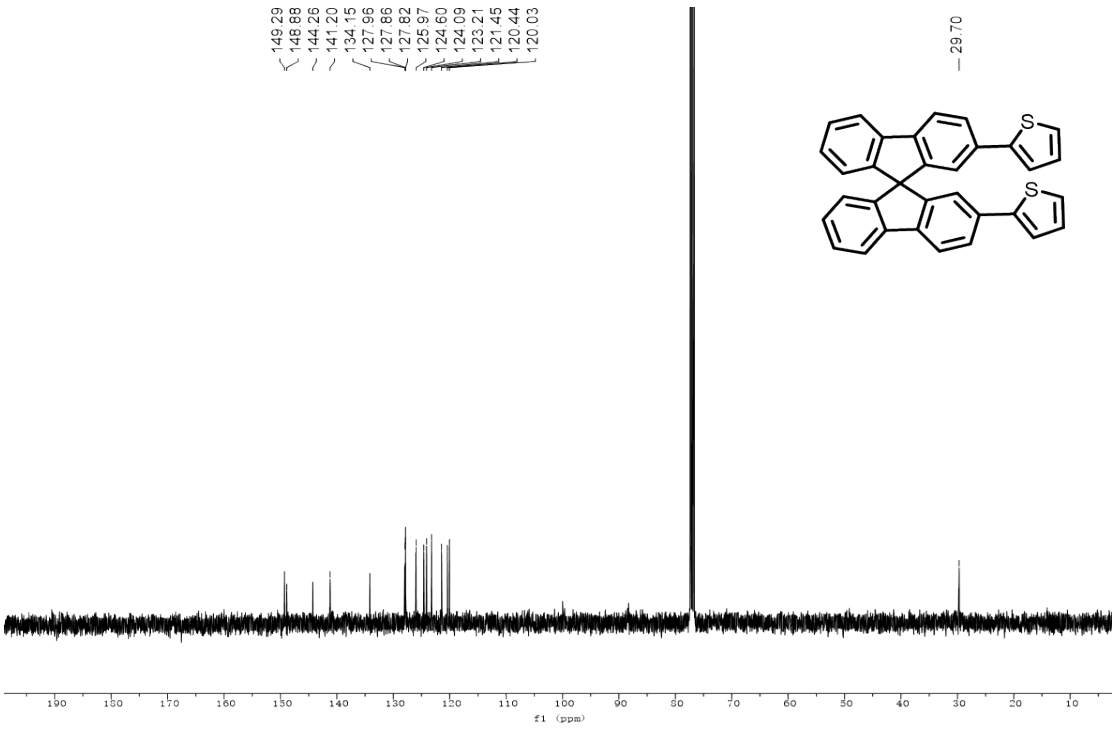

Fig. S29 ^{13}C NMR (100MHz, $CDCl_3$) spectrum of B_2.

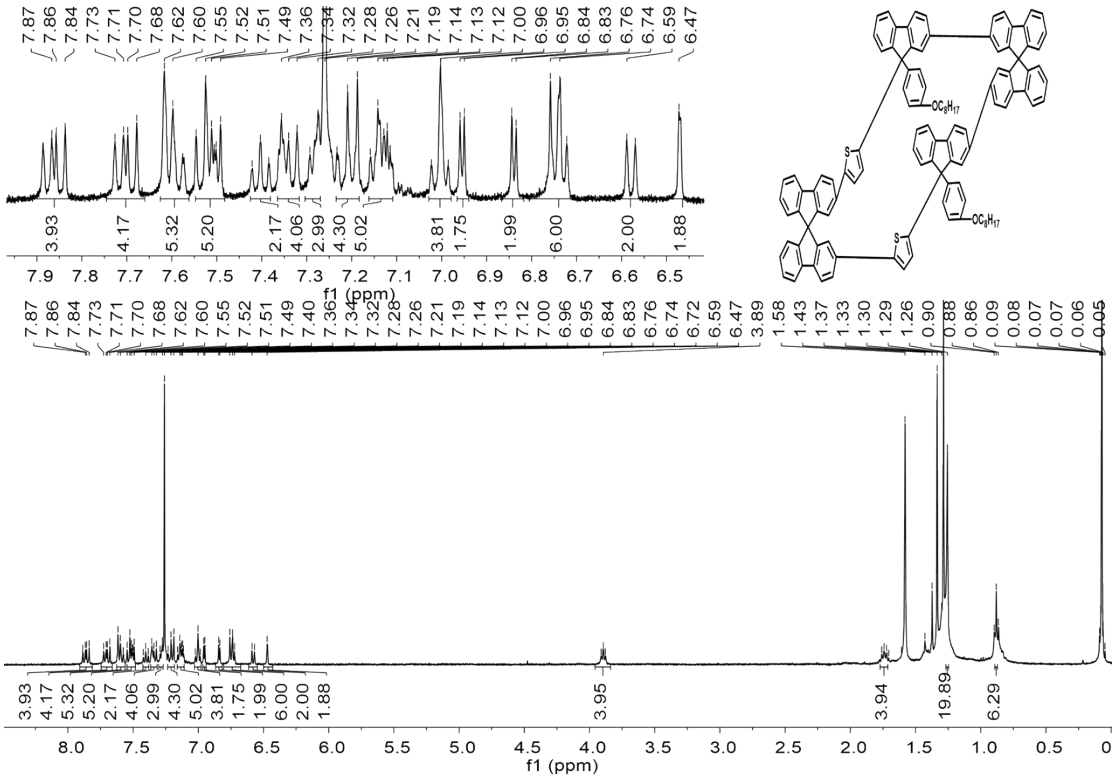

Fig. S30 ^{1}H NMR (400MHz, $CDCl_3$) spectrum of DGs-2.

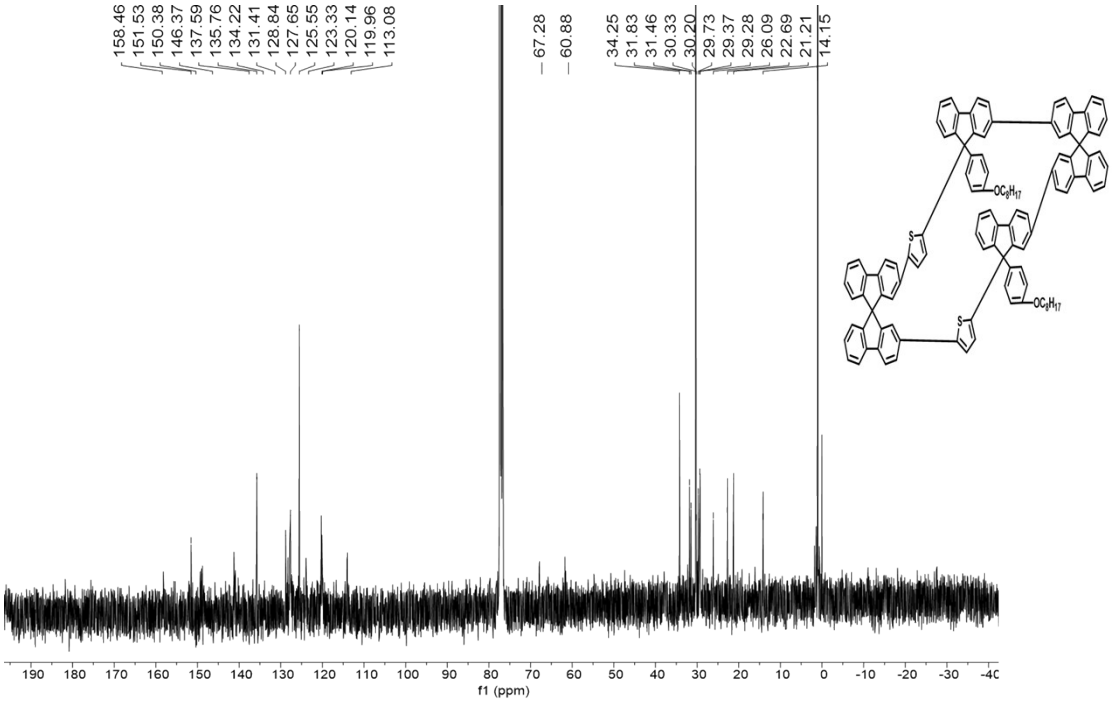

Fig. S31 ^{13}C NMR (100MHz, $CDCl_3$) spectrum of DGs-2.

7. MALDI-TOF-MS of compounds.

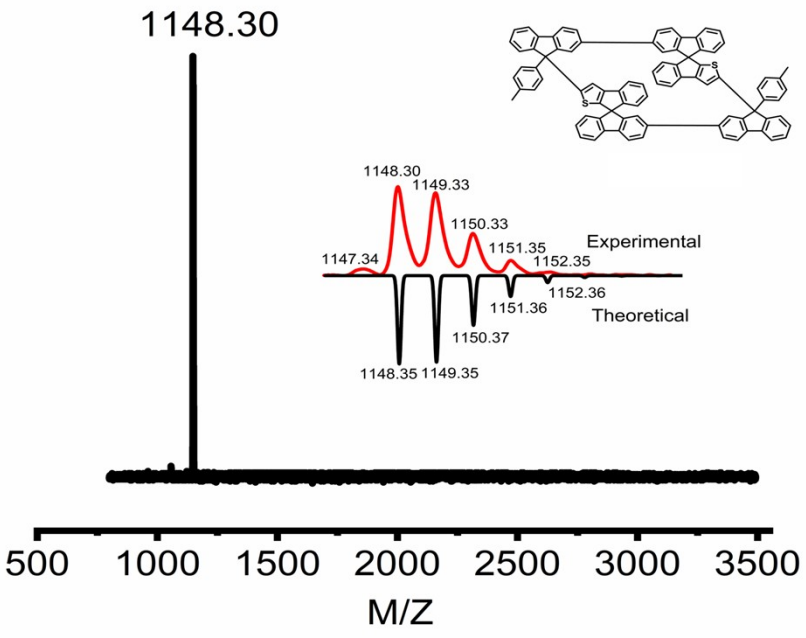

Fi

g. S32 The MALDI-TOF spectrum of DGs-1a.

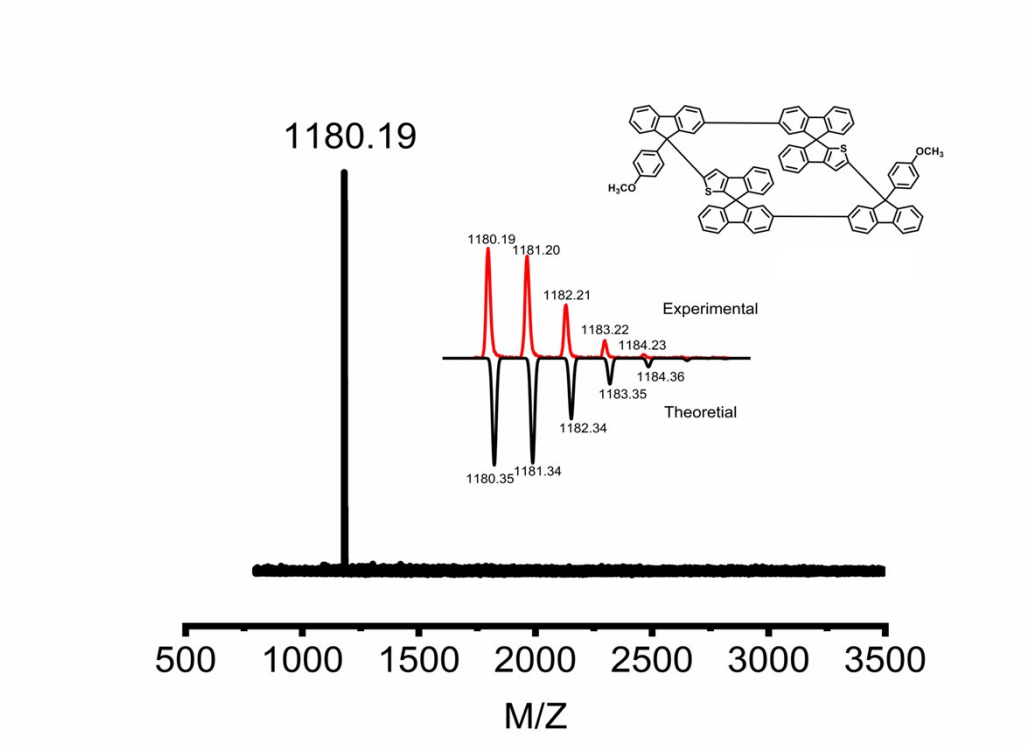

Fig. S33 The MALDI-TOF spectrum of DGs-1b.

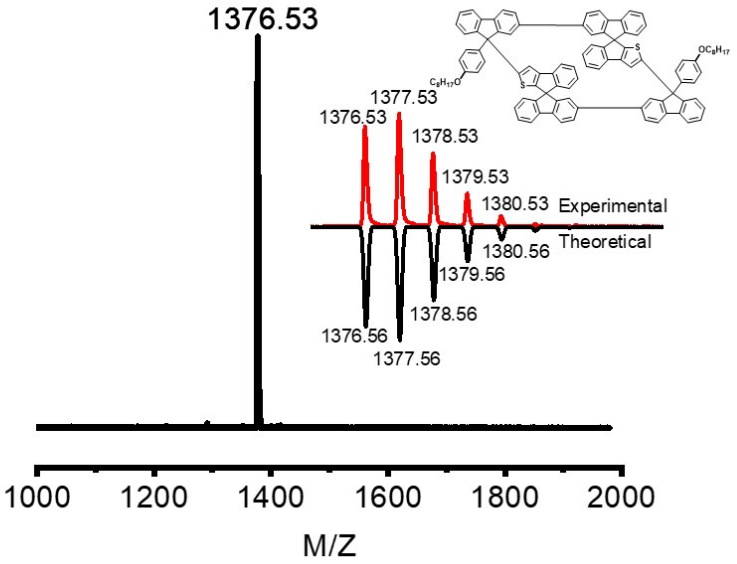

Fig. S34 The MALDI-TOF spectrum of DGs-1c.

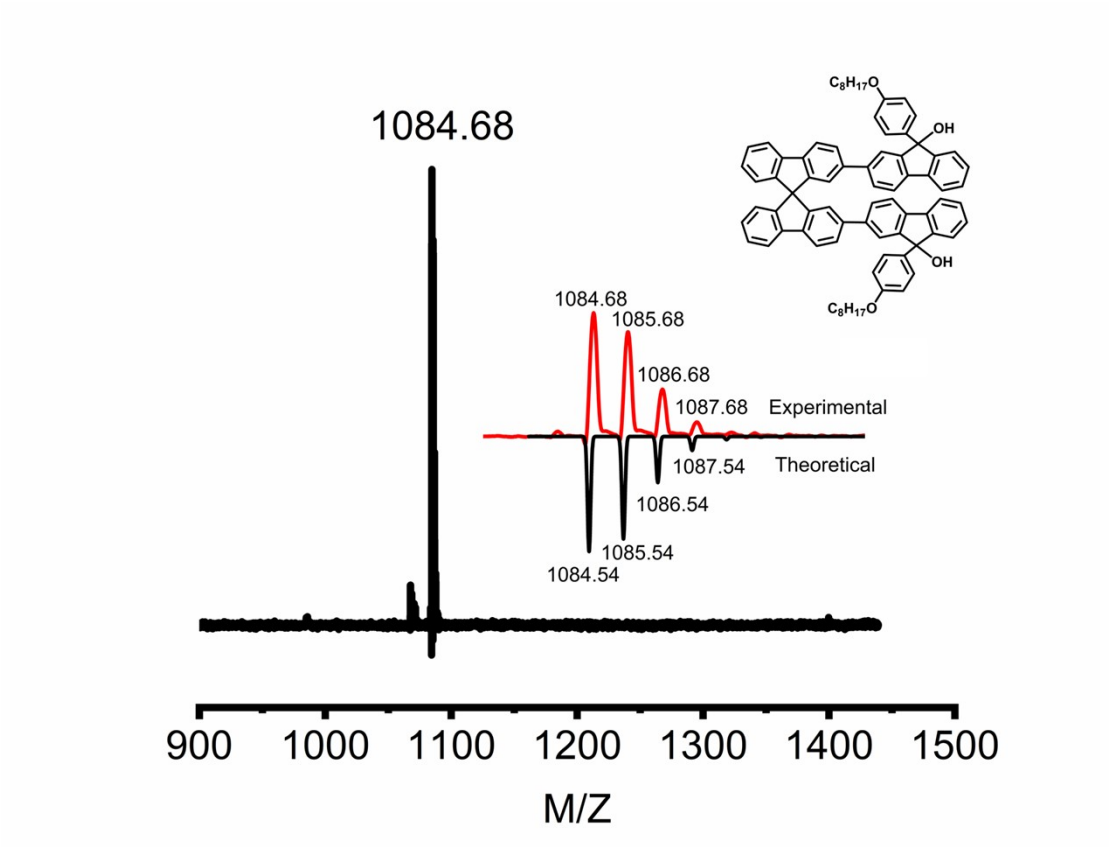

Fig. S35 The MALDI-TOF spectrum of A_2.

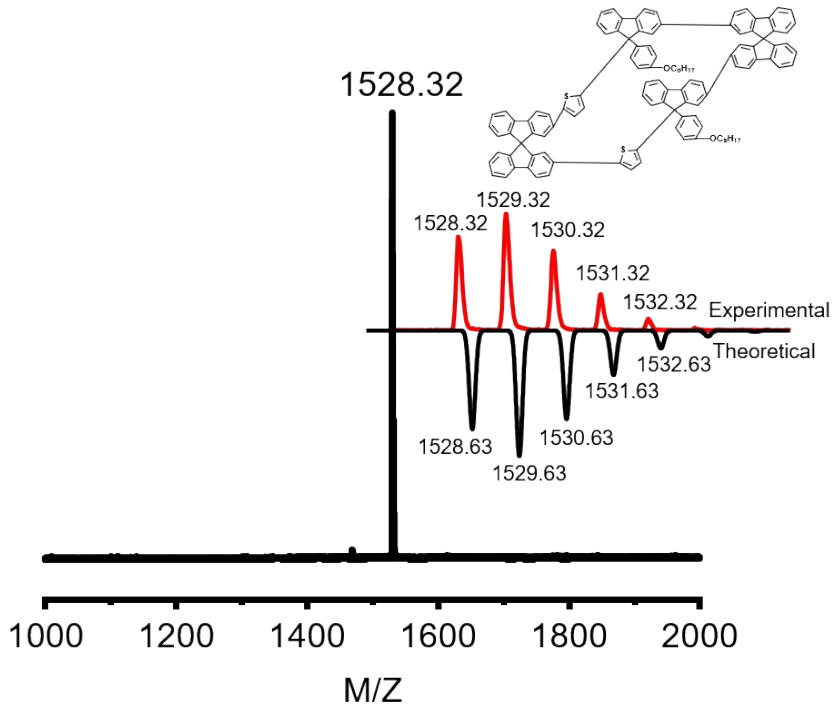

Fig. S36 The MALDI-TOF spectrum of DGs-2.